

# Rheological Behavior of Aciculate Ultrafine $\alpha$ -FeOOH Particles under Alkaline Conditions<sup>1</sup>

Chunzhong Li,<sup>2</sup> Shiyin Cai, and Tunan Fang

*Institute of Technical Chemistry and Physics, East China University of Science and Technology, P.O. Box 258, 130 Meilong Road, Shanghai 200237, Peoples' Republic of China*

Received October 13, 1997; in revised form February 26, 1998; accepted May 26, 1998

**The three-phase oxidation of ferrous hydroxide slurry can produce goethite ( $\alpha$ -FeOOH) iron oxide particles suitable for use in magnetic recording media. Experimental studies show that the reaction slurries were Newtonian liquids with a viscosities lower than 0.005 Pa·s at the beginning of the oxidation reaction. The reactive slurries displayed strong shear-thinning behavior, which can be fitted to a power law equation at the middle and later stages of reaction, and these slurries showed no thixotropy but showed a yield stress at quietus. The rheological behavior of the reaction slurries was mainly caused by the formation mechanism of  $\alpha$ -FeOOH particles and by the morphology change of the solid particles. The rheological behavior was strongly affected by dopants such as  $\text{MnSO}_4$ ,  $\text{MgSO}_4$ , and  $\text{Na}_2\text{SiO}_3$ . The apparent reaction rate was controlled by the oxygen mass transfer rate, which was strongly affected by the rheological behavior of the reactive slurries.** © 1998 Academic Press

## INTRODUCTION

Iron oxides are used in a wide variety of applications, including pigments and magnetic media. In most commercial processes, goethite ( $\alpha$ -FeOOH) particles are produced as an intermediate in the iron oxide preparation (1–4). The goethite crystals grow in the form of acicular needles about 0.1–1  $\mu\text{m}$  long with an aspect ratio of 5–15. For magnetic media, the desired product should be of uniform length and uniform but high aspect ratio. The goethite is then reacted through a series of gas–solid reactions to form  $\gamma$ - $\text{Fe}_2\text{O}_3$ . The goethite particle morphology is a critical factor in determining the magnetic properties of the  $\gamma$ - $\text{Fe}_2\text{O}_3$  particles (5).

There are two stages in the formation of goethite under alkaline conditions (6). In step one, ferrous sulfate (or any other ferrous salt) is mixed with excess NaOH (or some

other base such as KOH) so that ferrous hydroxide precipitate immediately forms. The amount of excess NaOH used is between 15 and 200% above the stoichiometric requirements. In step two, an oxygen-containing gas is bubbled through the slurry to form  $\alpha$ -FeOOH particles for controlling the synthesis conditions. The mechanisms involved in the oxidation reaction and crystal growth are very complex and generally not well understood (7–11). In many examples of particle formations, the morphology control has been individually met based on many years of experience (10, 11). However, if the physicochemical significance of the empirical method could be elucidated and the mechanism of particle formation clarified, then a more rational production process could be designed, instead of relying on empirical experience. Furthermore, both selection of optical reactor and optimal determination of operating conditions would become possible.

Currently, there is little work that has been done on mass transfer, especially on the rheological behavior of  $\alpha$ -FeOOH particle preparation. As a result, the formation of particles with the proper characteristics is often difficult in production-scale equipment. In this research, the rheological properties of the  $\alpha$ -FeOOH synthesis process of aciculate ultrafine  $\alpha$ -FeOOH particles are investigated, and the relationship of the rheological properties to the formation mechanism of  $\alpha$ -FeOOH particles is discussed.

## EXPERIMENTAL

The starting materials for  $\alpha$ -FeOOH synthesis were ferrous sulfate ( $\text{FeSO}_4 \cdot 7\text{H}_2\text{O}$ ), sodium hydroxide, and deionized water. The synthesis of  $\alpha$ -FeOOH particles was carried out in a 100-dm<sup>3</sup> open stirring reactor at 1-atm pressure. The suspensions of ferrous hydroxide were prepared by adding various amounts of a sodium hydroxide solution (45 dm<sup>3</sup>) to a ferrous sulfate solution (45 dm<sup>3</sup>) with constant stirring. The initial content of Fe(II) in ferrous solution was 0.72 mol·dm<sup>-3</sup>. The alkali molar ratio, defined by  $R = [\text{NaOH}]_0/2[\text{FeSO}_4]_0$ , was varied from 1.5 to

<sup>1</sup> Project 29636010 supported by the National Natural Science Foundation of China.

<sup>2</sup> To whom correspondence should be addressed. E-mail: czli@npc.haplinc.com.cn.

3.5 (but mainly set at 2.45). After the sodium hydroxide solution was fed into the stirring reactor, the aqueous solution was dispersed in air at a prescribed rate  $Q$  and stirred at a suitable temperature  $T$  to precipitate aciculate ultrafine  $\alpha$ -FeOOH particles. The air flow rate  $Q$ , reaction temperature  $T$ , and stirring rate  $n$  were controlled at  $800 \text{ dm}^3 \cdot \text{h}^{-1}$ ,  $40^\circ\text{C}$ , and  $40 \text{ rer} \cdot \text{min}^{-1}$ , respectively. Dopants, such as  $\text{MnSO}_4$ ,  $\text{MgSO}_4$ , and  $\text{Na}_2\text{SiO}_3$ , were added to the reaction slurry at different times. The oxidation reaction was followed by sampling a desired amount ( $100 \text{ cm}^3$ ) of reaction suspension periodically for determining the rheological properties, the morphology of the solid particles, and the concentration of Fe(II) in the reaction slurry.

The ferrous ion content was determined by potassium dichromate titration after the sample had been dissolved in phosphonic acid solution. The structure and morphology of the solid particles in the reaction slurry were examined by transmission electron microscopy (TEM, H-300). The rheological behavior of the reactive slurries at different times was measured with an RFS-II rheogoniometer with a concentric bob and cup measuring system. Rheological behavior measurements were made over a shear rate range of  $0.05\text{--}300 \text{ s}^{-1}$  and at temperatures between  $20$  and  $40^\circ\text{C}$ . The temperature remained constant during an experiment to within  $\pm 0.2^\circ\text{C}$ .

## RESULTS AND DISCUSSION

### Rheological Behavior

Plots of apparent viscosity as a function of shear rate ( $20^\circ\text{C}$ ) for the slurries at different reaction times are shown in Fig. 1. The reaction slurries at different times displayed different rheological behaviors. Over the range of shear rates studied, the slurries were non-Newtonian, with

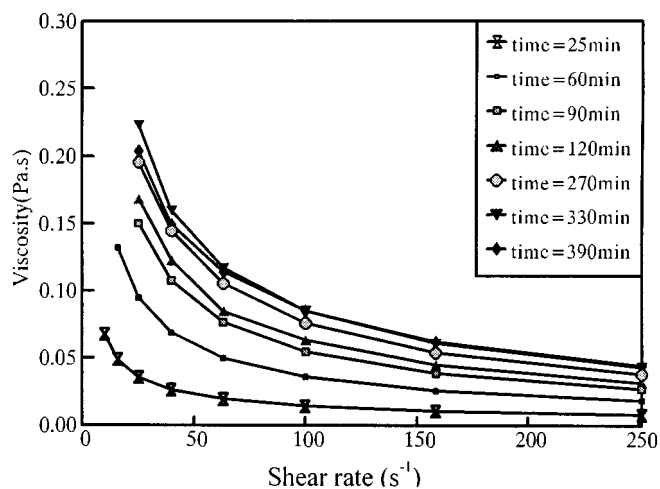


FIG. 1. Plots of apparent viscosity as a function of shear rate ( $20^\circ\text{C}$ ) for the slurries at different reaction times.

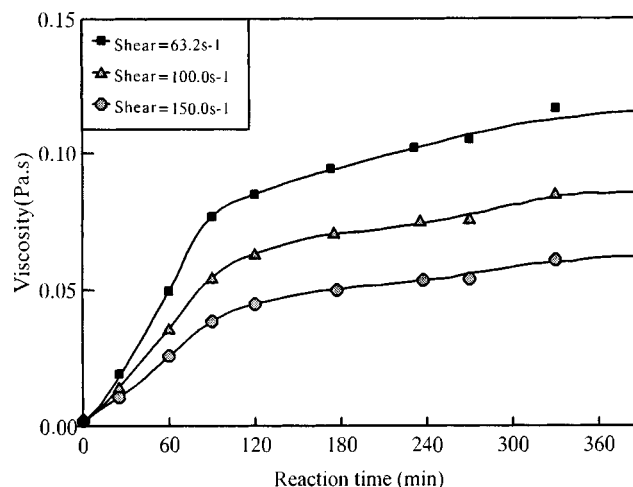


FIG. 2. Apparent viscosity of the reaction slurry at different reaction times and different shear rates.

shear-thinning behavior at the middle to later reaction stages, where the reaction slurries showed strong shear-thinning behavior at low shear rates but less shear-thinning behavior at high shear rates. The reaction slurries also displayed less shear-thinning behavior with low viscosity at the initial reaction stage. It should be noted that the shear rates in the same commercial stirring reactor vary considerably in different regions. In regions of low shear rate, the viscosity is high, which leads to a low mass transfer rate. Whereas in regions of large shear rate, the viscosity is low, which results in a high mass transfer rate. The difference of viscosity and mass transfer rate at different regions leads to a nonuniform reaction rate in the stirring reactor.

Figure 2 shows that the reaction slurry was a Newtonian liquid with low viscosity before the oxidation reaction began. The apparent viscosity was less than  $0.005 \text{ Pa}\cdot\text{s}$  at the initial reaction stage but increased to higher than  $0.06 \text{ Pa}\cdot\text{s}$  at the middle to later stages when the shear rate was equal to  $150 \text{ s}^{-1}$ . The apparent viscosity increased little with reaction time at the middle to later reaction stages.

The apparent viscosities of the slurries at different shear rates can be fitted to the power law equation  $\eta_a = K\dot{\gamma}^{n-1}$ . Table 1 shows results from fitting the power law equation. For  $\alpha$ -FeOOH synthesis under alkaline conditions, it was found that  $n \ll 1$ , which indicated also that the reaction slurries showed strong shear-thinning behavior. Figure 3 shows that the thixotropy of the reaction slurries was not significant because the hysteresis loops were very small. The stress overshoot at lower shear rate showed that there exists a yield stress of the reaction slurries at quietus.

The rheological behavior of the reaction slurries depends strongly on the formation mechanism of aciculate  $\alpha$ -FeOOH particles and on the morphology change of the solid particles. The electron micrographs in Fig. 4 illustrate

**TABLE 1**  
Parameters of Power Law for the Reaction Slurry of  $\alpha$ -FeOOH Synthesis

Reaction time (min)	Transition ratio	$K$	$n$	Correlation parameter
25	0.16	0.29	0.355	0.999
60	0.35	0.91	0.298	1.000
90	0.46	1.62	0.262	1.000
120	0.50	1.59	0.286	0.998
270	0.75	2.10	0.271	0.999
330	0.86	2.35	0.273	1.000
390	0.96	2.07	0.296	0.999

the time evolution of the solid phase aged under standard conditions. It is obvious from comparison between these electron micrographs that the initially observed spherical  $\text{Fe}(\text{OH})_2$  particles were gradually replaced by acicular  $\alpha$ -FeOOH particles. The formation of acicular  $\alpha$ -FeOOH particles and the change of solid particle morphology made the slurries at different reaction times display quite different

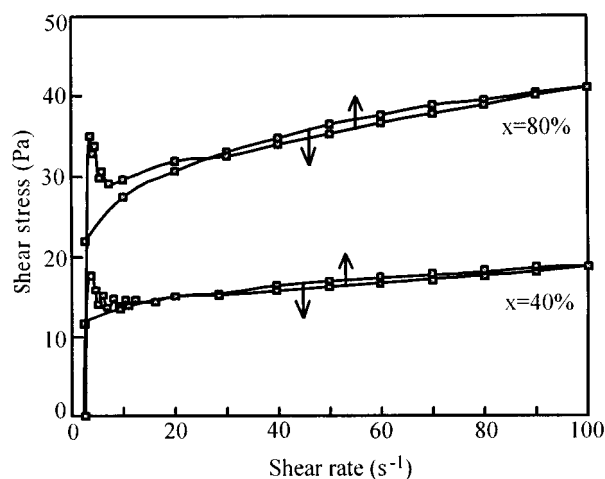


**FIG. 3.** Thixotropy of the reaction slurry for pure  $\alpha$ -FeOOH synthesis under alkaline conditions.

rheological behaviors, especially at low shear rates. Many studies have indicated that dispersions of acicular particles have a larger viscosity than those of spherical particles (12–15). This confirmed that the viscosity and the degree of

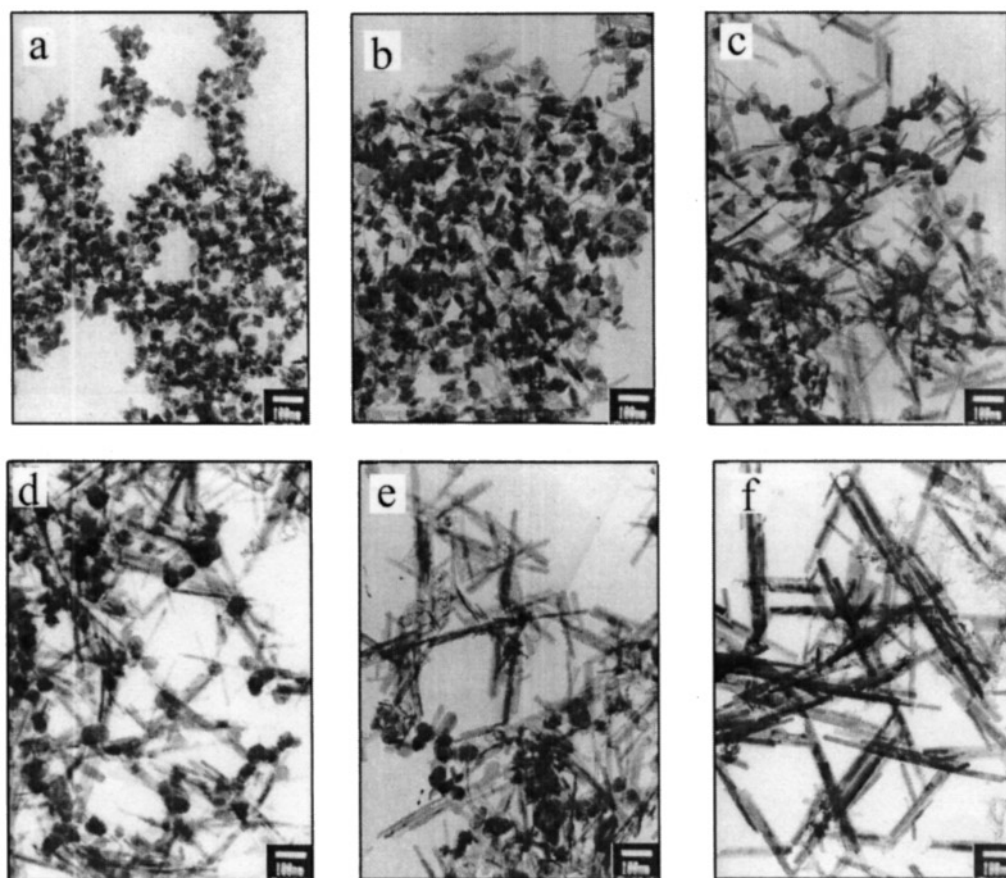


**FIG. 4.** Transmission electron micrographs of the solid particles in the reaction slurry at different reaction times: (a) 0 min; (b) 20 min; (c) 40 min; (d) 90 min; (e) 180 min; (f) 360 min.

shear-thinning increase rapidly when acicular  $\alpha$ -FeOOH particles are formed at the initial to middle reaction stages. At a later stage the viscosity and the degree of shear-thinning increase slowly because the morphology and numerical concentration of  $\alpha$ -FeOOH particles change little with reaction time.

### Effects of Dopants

The rheological behavior changes sharply if dopants such as  $\text{MnSO}_4$ ,  $\text{MgSO}_4$ , and  $\text{Na}_2\text{SiO}_3$  are added to the reaction slurry. The flow curves are given in Fig. 5. At the middle to later reaction stage, mainly when the oxidation fraction was larger than 0.4, the viscosity of the reaction slurries increased notably when  $\text{MnSO}_4$  was added before the air was passed through the reaction slurry. The studies of Li (16) and Du (17) indicated that, for  $\alpha$ -FeOOH particle synthesis under alkaline conditions, the particle size and aspect ratio of acicular  $\alpha$ -FeOOH particles increased by doping with  $\text{Mn}^{2+}$ . The morphology change of  $\alpha$ -FeOOH particles increased the particle interaction; as a result the viscosity of the reaction slurry increased notably at the middle to later reaction stage. Li (16) and Okada (18) observed that the particle morphology changed only slightly when  $\text{MgSO}_4$  was added to the  $\text{Fe}(\text{OH})_2$  suspension; thus the viscosity and the shear-thinning behavior changed little for the Mg-doped  $\alpha$ -FeOOH particle synthesis process.

The rheological behavior changed sharply and the viscosity decreased greatly with the addition of  $\text{Na}_2\text{SiO}_3$  to the reaction slurry. As shown in Fig. 5, the reaction slurry displayed different rheological behaviors when different amounts of  $\text{Na}_2\text{SiO}_3$  were added at different reaction times. The particle size and aspect ratio became smaller on doping with  $\text{Na}_2\text{SiO}_3$  at the initial reaction stage, as had been

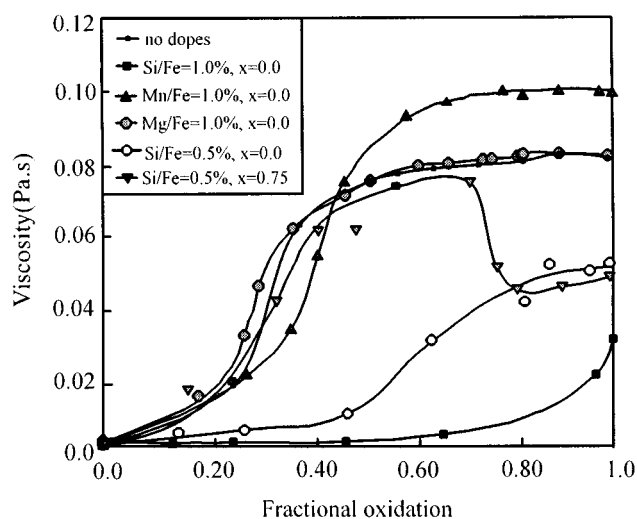


FIG. 5. Effects of dopants on the viscosity of the reaction slurry.

observed by Li (16, 19), Scheffer (20), Krause (21), and Schelmann (22). As the particle size and aspect ratio decreased, the linkages of particles became weaker and were more easily broken down by shear. Another reason for the change of rheological behavior is that  $\text{Na}_2\text{SiO}_3$  acts as surfactant for the reaction slurry. Many studies had indicated that  $\text{SiO}_3^{2-}$  was easily adsorbed on the surface of  $\text{Fe}(\text{OH})_2$  and  $\text{FeOOH}$  particles (19–23). The adsorption of  $\text{Na}_2\text{SiO}_3$  decreased the interaction of particles, which caused the decrease in viscosity.  $\alpha$ -FeOOH particle morphology changed little if  $\text{Na}_2\text{SiO}_3$  was added at the middle to later reaction stages (16, 19), but the viscosity decreased sharply. This phenomenon was attributed to the adsorption of  $\text{Na}_2\text{SiO}_3$ . For the synthesis of doped  $\alpha$ -FeOOH the reaction slurries showed a strong shear-thinning behavior, with no thixotropy, but yield stress set in when the slurry was stationary, which was somewhat the same as for the reactive slurry in the pure  $\alpha$ -FeOOH synthesis process. It should be borne in mind that many kinds of impurities in the raw materials exist in the particle synthesis. The impurities will affect the product particle morphology and rheological behavior of the reaction slurry. As a result, the formation of the particles with the proper characteristics (e.g., fine needles with a high aspect ratio and controlled size) is often difficult in production-scale equipment; a general quantitative approach to modeling the particle growth is not currently available.

### Mass Transfer Rate

The three-phase oxidation of ferrous hydroxide slurry can produce goethite ( $\alpha$ -FeOOH) iron oxide particles suitable for use in magnetic recording media. The studies of O'Connor (11) and Gu (24) showed that the apparent reaction rate for the oxidation of ferrous iron in an  $\text{Fe}(\text{OH})_2$  slurry is limited by the rate of mass transfer of oxygen into the liquid. At high slurry loadings, the mass transfer rate can change significantly with conversion, implying a change in viscosity. The time dependence of fractional oxidation of  $\text{Fe}(\text{II})$  at different doping conditions is shown in Fig. 6, where the air flow rate, stirring rate, alkali ratio, and the initial concentration of  $\text{Fe}(\text{II})$  were kept constant. As shown in Fig. 6, the apparent reaction rates of the Mg-doped, Mn-doped, and pure  $\alpha$ -FeOOH particle synthesis process decreased very sharply at initial stages, while the fractional oxidation increased linearly with time at the middle to later reaction stages. This trend of the apparent reaction rate can contribute to the change of the viscosity of the reactive slurry. At the initial reaction stage, the viscosity increased very sharply with the reaction time, whereas at the middle to later stages, the viscosity changed little with the reaction time.

For the Si-doped  $\alpha$ -FeOOH synthesis process, the changes of apparent reaction rate showed a different trend compared to the pure  $\alpha$ -FeOOH synthesis process. At the

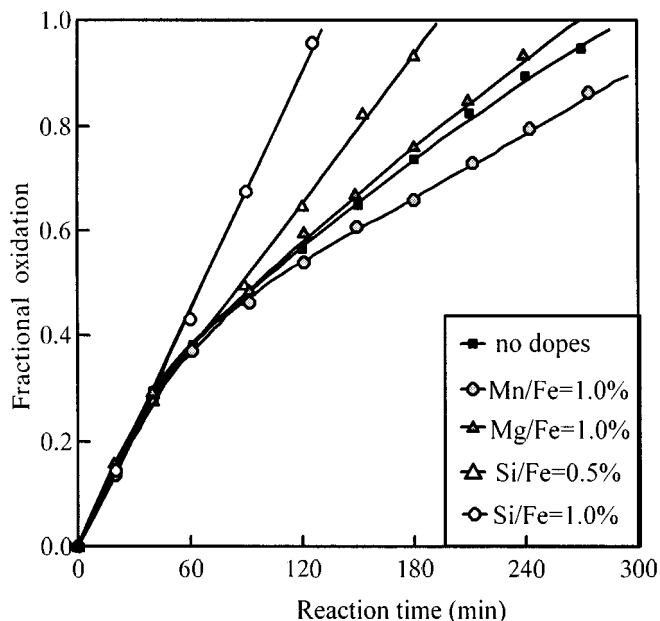


FIG. 6. Time dependence of fractional conversion of oxidation reaction of Mg-doped, Mn-doped, Si-doped, and pure  $\alpha$ -FeOOH particle synthesis process.

initial reaction stage the fractional oxidation of Fe(II) increased linearly because the viscosity changed little, whereas at the later reaction stage, the apparent reaction rate decreased greatly because the viscosity increased notably with reaction time.

### CONCLUSION

The reaction slurries displayed different rheological behaviors at different conversions. The reaction slurries constituted a Newtonian liquid with a viscosity lower than 0.005 Pa·s at the initial reaction stage. The reaction slurries displayed strong shear-thinning behavior which can be fitted to a power law equation at the middle to later stages, and these slurries exhibited yield stress at the quietus but without thixotropy. The rheological behavior of the reaction slurries was mainly caused by the formation mechanism of  $\alpha$ -FeOOH particles and by the morphology change of solid particles in the reaction slurries.

The rheological behavior was strongly affected by dopants added to the reaction slurries. The viscosity increased notably on adding  $\text{MnSO}_4$  but changed little on adding  $\text{MgSO}_4$  in the reaction slurries. The viscosity decreased very sharply by doping with  $\text{Na}_2\text{SiO}_3$ ; this

phenomenon was attributed to the adsorption on the surface of solid particles and to the decrease of the particle size and aspect ratio of the  $\alpha$ -FeOOH particles.

For the three-phase oxidation of ferrous hydroxide, the apparent reaction rate was limited by the rate of mass transfer of oxygen into the liquid. The apparent reaction rate for the Mg-doped, Mn-doped, and pure  $\alpha$ -FeOOH particle synthesis process decreased with the fractional oxidation at the initial reaction stage but changed little at the middle to later reaction stages. The apparent reaction rate displayed a contrary trend if  $\text{Na}_2\text{SiO}_3$  was added at the initial reaction stage.

### REFERENCES

1. M. P. Sharrock and R. E. Bodnar, *J. Appl. Phys.* **57**, 3919 (1985).
2. L. M. Bennetch, H. S. Greiner, K. R. Hancock, and M. Hoffman, U. S. Patent 3904540, 1975.
3. H. Sesigur, E. Acma, O. Addemir, and A. Tekin, *Mater. Res. Bull.* **31**, 1573 (1996).
4. H. Kopke, M. Ohlinger, W. Grau, E. Schoenafinger, and H. H. Schneehage, U. S. Patent 4059716, 1977.
5. E. P. Wohlfarth, "Ferromagnetic Materials: A Handbook of the Properties of Magnetically Ordered Substances," Vol. 2. Elsevier, North-Holland, Amsterdam, 1980.
6. T. Misawa, K. Hashimoto, and S. Shimodara, *Corros. Sci.* **14**, 131 (1974).
7. W. Feitknecht, *Z. Elektrochem.* **63**, 34 (1959).
8. Y. Tamaura, *M. Chem. Soc., Dalton Trans.* **197**, 1807 (1981).
9. W. Feitknecht and P. Schindler, *Pure Appl. Chem.* **6**, 134 (1963).
10. E. Sada, H. Kumazawa, and M. Aoyama, *Chem. Eng. Commun.* **71**, 73 (1988).
11. D. L. O'Connor, M. P. Dudukovic, and P. A. Ramachandran, *Ind. Eng. Chem. Res.* **31**, 2516 (1992).
12. H. A. Barnes, J. F. Hutton, and K. Walters, "An Introduction to Rheology," Chap. 7. Elsevier, Amsterdam, 1989.
13. B. Clarke, *Trans. Inst. Chem. Eng.* **45**, 251 (1967).
14. R. Turian and T.-F. Yuan, *AIChEJ.* **23**, 232 (1977).
15. H. Giesekus, "Physical Properties of Foods," (R. Jowitt *et al.*, Eds.), Chap. 13. Applied Science Publishers, London, 1983.
16. C. Li, Morphology Control and Process Study on Ultrafine Magnetic Powder Preparation, Section 2 Doctoral Thesis, East China University of Science and Technology, Shanghai, 1996.
17. Y. Du and H. Luo, "Magnetic Recording Materials." Electron Industry Press, Peking, 1992.
18. Y. Okada, U. S. Patent 4495164, 1984.
19. C. Li, Y. Zhu, A. Ce, and H. Gu, *J. East China Univ. Sci. Technol.* **23**, 571 (1997).
20. F. Scheffer, *Chem. Erde* **19**, 51 (1957).
21. A. Krause and A. Borkowska, *Monatsh. Chem.* **94**, 460 (1963).
22. W. Schellmann, *Chem. Erde* **20**, 104 (1959).
23. K. Kandori, S. Uchida, S. Kataoka, and T. Ishikawa, *J. Mater. Sci.* **27**, 719 (1992).
24. H. Gu, J. Chen, and L. Hu, *J. East China Univ. Sci. Technol.* **18**, 472 (1992).